

# Magnetic properties of hydrothermally synthesized strontium hexaferrite as a function of synthesis conditions

A. ATAIE, I. R. HARRIS, C. B. PONTON\*

*School of Metallurgy and Materials, \*and also IRC in Materials for High Performance Applications, The University of Birmingham, Edgbaston, Birmingham, B15 2TT, UK*

Fine particles of strontium hexaferrite,  $\text{SrFe}_{12}\text{O}_{19}$ , with a narrow size distribution have been synthesized hydrothermally from mixed aqueous solutions of iron and strontium nitrates under different synthesis conditions. The relationship between the synthesis variables (temperature, time and alkali molar ratio) and the magnetic properties has been investigated. The results have shown that, as the synthesis temperature increases, the saturation magnetization of the particles increases up to a plateau and the coercivity decreases. As the alkali molar ratio  $R(=\text{OH}^-/\text{NO}_3^-)$  increases, the coercivity decreases and goes through a local minimum, while the saturation magnetization increases and goes through a local maximum. Increasing the synthesis time from 2 h to 5 h has no significant effect on the saturation magnetization, but decreases the coercivity. An anisotropic sintered magnet with a high saturation magnetization value of  $67.26 \text{ e.m.u. g}^{-1}$  ( $4320 \text{ G}$ )<sup>†</sup> has been fabricated from the hydrothermally synthesized powders.

## 1. Introduction

The principle characteristics of and preparation methods for strontium hexaferrite have been reviewed by Kojima [1] and Stäblein [2], respectively. Strontium hexaferrite,  $\text{SrFe}_{12}\text{O}_{19}$ , possesses a high coercivity owing to its relatively high magnetocrystalline anisotropy field ( $H_A = 20 \text{ kOe}$ ) and this property makes it an attractive material for use in permanent magnet applications [1]. Strontium hexaferrite is produced mainly by a conventional mixed oxide ceramic method which involves calcining of  $\text{SrCO}_3$  and  $\alpha\text{Fe}_2\text{O}_3$  at around  $1200^\circ\text{C}$ . However, in order to improve the material properties, non-conventional routes, such as the coprecipitation method [3–5], organometallic precursor method [6], glass crystallization method [7, 8], salt-bath method [9] and the hydrothermal method [10, 11], have been also employed to synthesize strontium hexaferrite. Recently, the authors have synthesized uniform-size high-purity strontium hexaferrite particles of plate-like morphology at a relatively low temperature of  $200^\circ\text{C}$  for a short time of 1 h, and investigated systematically the effects of the synthesis conditions on the sol particle morphology and crystal structure [11].

In the present paper, the effects of the synthesis conditions on the magnetic properties have been studied in more detail. The fabrication of sintered magnets from these powders has also been investigated.

## 2. Experimental procedure

Aqueous solutions of strontium and iron nitrates were coprecipitated by the addition of  $\text{NaOH}$  (aq) in different  $\text{OH}^-/\text{NO}_3^-$  molar ratios (from 1.5–7) and subsequently the precipitated solutions were processed in an autoclave (a 250 ml PTFE-lined Berghof laboratory autoclave) at different temperatures and times. The details of the synthesis procedure have been described previously [11]. A slurry of the particles synthesized at  $220^\circ\text{C}$  for 1 h with an  $\text{OH}^-/\text{NO}_3^-$  molar ratio of 2 (without any additives) was pressed using a Hiton hydraulic press at a pressure of 68.5 MPa in a magnetic field strength of about  $10^4 \text{ G}$  (1T). The resultant green compacts were dried overnight in an oven at  $50^\circ\text{C}$  and then one was sintered at  $1200^\circ\text{C}$  for 1 h and the other at  $1250^\circ\text{C}$  for 1 h in a programmed muffle furnace with heating and cooling rates of  $3^\circ\text{C min}^{-1}$ ; see Section 3.4. Densities of the fabricated magnets were measured by the displacement method using diethyl phthalate [ $\text{C}_6\text{H}_4(\text{COO} \cdot \text{C}_2 \cdot \text{H}_5)_2$ ] with a density  $1.1298 \text{ g cm}^{-3}$  at  $8^\circ\text{C}$ , as the immersion liquid.

X-ray powder diffraction (cobalt radiation), scanning electron microscopy (SEM), and vibrating sample magnetometer (VSM) measurements (at a maximum field of 14 kOe) have been used to analyse the phase composition, morphology and magnetic properties of the particles, respectively. The microstructures of the

<sup>†</sup>Relationship between the c.g.s and S.I. units which are used in this paper are as follows:  $1 \text{ erg} = 10^{-7} \text{ J}$ ,  $1 \text{ e.m.u. cm}^{-3} = 12.57 \times 10^{-7} \text{ Wbm}^{-2}$  (tesla),  $1 \text{ oersted (Oe)} = 79.6 \text{ A m}^{-1}$ ,  $1 \text{ G} = 10^{-4} \text{ tesla (T)}$ .

sintered magnets were studied using optical microscopy after etching them in 50 % HCl at 80 °C.

### 3. Results and discussion

#### 3.1. Effect of synthesis time

The powder X-ray diffraction patterns for strontium hexaferrite synthesized hydrothermally at 220 °C with an  $\text{OH}^-/\text{NO}_3^-$  molar ratio of 2 for synthesis times of 0.5, 1, 2 and 5 h, confirmed the formation of strontium hexaferrite even after only 0.5 h synthesis time [11]. Fig. 1 shows a scanning electron micrograph of hexagonal and plate-like particles of strontium hexaferrite synthesized under the above conditions for 0.5 h.

The saturation magnetization,  $\sigma_s$ , and intrinsic coercivity,  $H_{ci}$ , of strontium hexaferrite (synthesized hydrothermally at a temperature of 220 °C with an  $\text{OH}^-/\text{NO}_3^-$  molar ratio of 2) are shown in Fig. 2 as a function of synthesis time. It appears that the coercivity decreases with increasing synthesis time due to an increase in the particle size. The saturation magnetization,  $\sigma_s$ , increases significantly with increasing synthesis time from 0.25–2 h, but then changes little for longer times.

These results confirm the observations that the nucleation and growth of  $\text{SrFe}_{12}\text{O}_{19}$  crystals are completed within 2 h under the given experimental conditions. The existence of some intermediate precipitates such as  $\alpha\text{Fe}_2\text{O}_3$  (less than 10 wt % of which cannot be

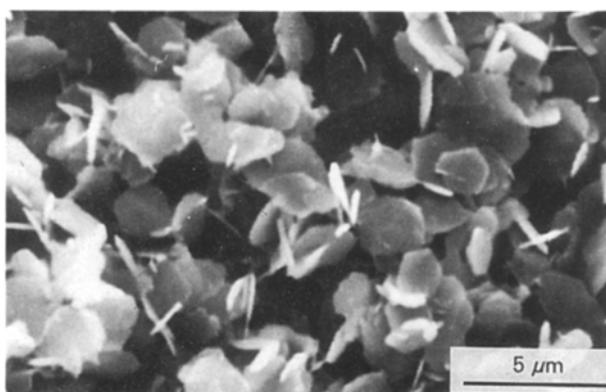


Figure 1 Scanning electron micrograph of strontium hexaferrite synthesized hydrothermally for 0.5 h at a temperature of 220 °C with a  $\text{OH}^-/\text{NO}_3^-$  molar ratio of 2.

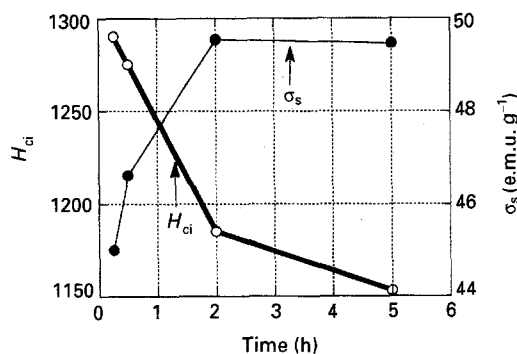


Figure 2 Saturation magnetization,  $\sigma_s$ , and intrinsic coercivity,  $H_{ci}$ , of strontium hexaferrite synthesized hydrothermally at a temperature of 220 °C with an  $\text{OH}^-/\text{NO}_3^-$  molar ratio of 2 as a function of synthesis time.

identified by the powder X-ray diffraction method) and the low crystallinity of the  $\text{SrFe}_{12}\text{O}_{19}$  particles are probably responsible for the relatively low saturation magnetization values of the samples synthesized for 0.25 and 0.5 h.

#### 3.2. Effect of $\text{OH}^-/\text{NO}_3^-$ molar ratio

Fig. 3 shows the powder X-ray diffraction patterns for strontium hexaferrite synthesized hydrothermally at 220 °C for 5 h with  $\text{OH}^-/\text{NO}_3^-$  molar ratios,  $R$ , of 1.5, 2, 3, 5, 6 and 7. Note that, owing to differences between the relative line intensities, the three lower graphs are plotted on a different intensity scale to the upper three patterns.

The amount of  $\text{SrFe}_{12}\text{O}_{19}$  present decreased dramatically on decreasing the  $\text{OH}^-/\text{NO}_3^-$  molar ratio from 2 to 1.5, owing to the presence of a high proportion of intermediate precipitates such as iron oxide. The powder composition does not appear to be influenced significantly by an  $\text{OH}^-/\text{NO}_3^-$  molar ratio in the range of 2–7. The characteristics of the prepared particles as a function of  $\text{OH}^-/\text{NO}_3^-$  molar ratio are shown in Table I.

Fig. 4 shows the saturation magnetisation,  $\sigma_s$ , and intrinsic coercivity,  $H_{ci}$ , of strontium hexaferrite synthesized hydrothermally at 220 °C for 5 h as a function of  $\text{OH}^-/\text{NO}_3^-$  molar ratio. As the  $\text{OH}^-/\text{NO}_3^-$  molar ratio increases from 1.5 to 2, the coercivity drops from 1970 Oe to 1153 Oe and then decreases slightly with increasing molar ratio up to 5. The coercivity is decreased noticeably at a molar ratio of 6 but increases slightly at a molar ratio of 7. The decrease in the

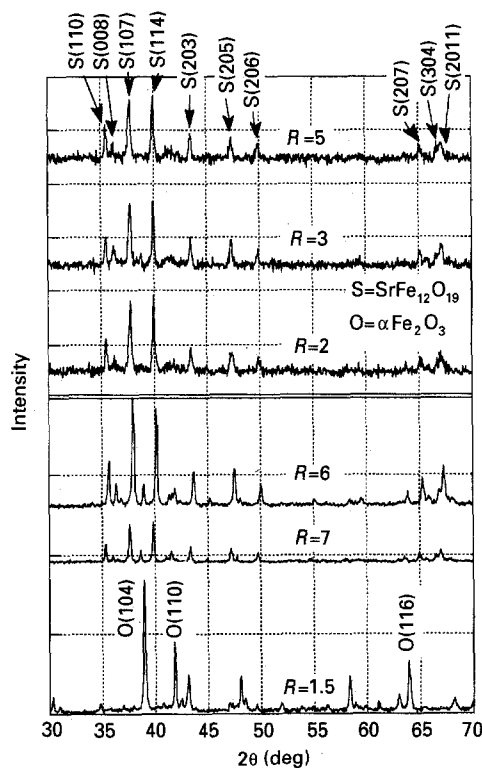


Figure 3 Powder X-ray diffraction patterns of strontium hexaferrite synthesized hydrothermally at 220 °C for 5 h as a function of  $\text{OH}^-/\text{NO}_3^-$  molar ratio,  $R$ .

TABLE I Average particle diameter,  $d$ , thickness,  $t$  and aspect ratio,  $d/t$ , and the intrinsic coercivity,  $H_{ci}$ , remanence,  $\sigma_r$ , and saturation magnetization,  $\sigma_s$ , of strontium hexaferrite synthesized hydrothermally at 220 °C for 5 h as a function of  $\text{OH}^-/\text{NO}_3^-$  molar ratio,  $R$

$\text{OH}^-/\text{NO}_3^-$ , $R$	$d$ ( $\mu\text{m}$ )	$t$ ( $\mu\text{m}$ )	$d/t$	$H_{ci}$ (Oe)	$\sigma_r$ (e.m.u. g $^{-1}$ )	$\sigma_s$ (e.m.u. g $^{-1}$ )
1.5	1.5	0.3	5	1972	1.25	2.89
2	1.68	0.24	7	1153	16.79	49.46
3	1.80	0.32	5.6	1070	15.57	48.85
5	1.83	0.32	5.7	1061	16.13	50.64
6	5.8	1	5.8	674	12.98	57.57
7	4.5	0.6	7.5	734	13.48	50.14

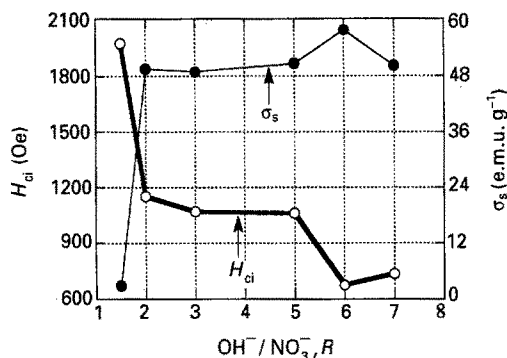


Figure 4 Saturation magnetization,  $\sigma_s$ , and intrinsic coercivity,  $H_{ci}$ , as a function of  $\text{OH}^-/\text{NO}_3^-$  molar ratio for strontium hexaferrite synthesized hydrothermally at 220 °C for 5 h.

coercivity, which is due to an increase in the particle size (as shown in Table I), confirms that increasing the concentration of the alkali up to  $R = 6$  results in an increased particle growth rate. However, at  $R = 7$  the rate is reduced. The saturation magnetization increases rapidly as  $R$  increases from 1.5 to 2, and increases to a local maximum at  $R = 6$ . The relatively low value of the saturation magnetization for the sample synthesized using an alkali molar ratio of 1.5 can be attributed to the presence of intermediate phases. Negligible magnetic properties were achieved for sample synthesized at  $R = 8$ .

In agreement with the XRD analysis, no significant change occurs in the saturation magnetization of samples synthesized using an alkali molar ratio in the range 2–7, except for the sample synthesized using an  $\text{OH}^-/\text{NO}_3^-$  molar ratio of 6 which exhibits a relatively high saturation magnetization corresponding to a high purity and maximum particle size. The above results indicate that the proportion of  $\text{SrFe}_{12}\text{O}_{19}$  formed increases markedly on increasing the  $\text{OH}^-/\text{NO}_3^-$  molar ratio,  $R$ , from 1.5 to 2 but remains relatively constant between  $R = 2$  and 3; it then increases when  $R$  is increased to 6. However, the proportion is then decreased at a ratio of 7. Increasing the alkali molar ratio from 6 to 7 appears to negate the catalytic effect of NaOH on the conversion of the strontium and iron nitrate precursors to  $\text{SrFe}_{12}\text{O}_{19}$ . This is due, possibly, to a now deleterious number of  $\text{Na}^+$  ions in the system, i.e. the excess  $\text{Na}^+$  ions above a critical concentration may hinder, rather than catalyse, the nitrate conversion process. Barium hexaferrite showed similar behaviour at a relatively high range of pH [12].

The scanning electron micrograph in Fig. 5 shows the relatively large, plate-like particles of strontium hexaferrite synthesized at 220 °C for 5 h using an  $\text{OH}^-/\text{NO}_3^-$  molar ratio of 6.

### 3.3. Effect of synthesis temperature

The particle characteristics (diameter, thickness and aspect ratio) and magnetic properties (coercivity, remanence and saturation magnetization) of  $\text{SrFe}_{12}\text{O}_{19}$  particles synthesized at 160, 180, 200 and 220 °C for 1 h using an  $\text{OH}^-/\text{NO}_3^-$  molar ratio of 2 are shown in Table II.

Fig. 6 shows the saturation magnetization,  $\sigma_s$ , and intrinsic coercivity,  $H_{ci}$ , of strontium hexaferrite

TABLE II The average particle diameter,  $d$ , thickness,  $t$ , and aspect ratio,  $d/t$ , and the intrinsic coercivity,  $H_{ci}$ , remanence,  $\sigma_r$ , and saturation magnetization,  $\sigma_s$ , of strontium hexaferrite particles synthesized hydrothermally for 1 h using an  $\text{OH}^-/\text{NO}_3^-$  molar ratio of 2 as a function of synthesis temperature [11]

Temp. (°C)	$d$ ( $\mu\text{m}$ )	$t$ ( $\mu\text{m}$ )	$d/t$	$H_{ci}$ (Oe)	$\sigma_r$ (e.m.u. g $^{-1}$ )	$\sigma_s$ (e.m.u. g $^{-1}$ )
160	0.7	0.3	2.3	1783	0.9	2.47
180	0.9	0.2	4.5	1643	10.88	24.68
200	1.4	0.3	4.66	1453	20.97	48.53
220	1.68	0.24	7.0	1055	16.79	49.7



Figure 5 Scanning electron micrograph of strontium hexaferrite synthesized hydrothermally at 220 °C for 5 h using an  $\text{OH}^-/\text{NO}_3^-$  molar ratio of 6.

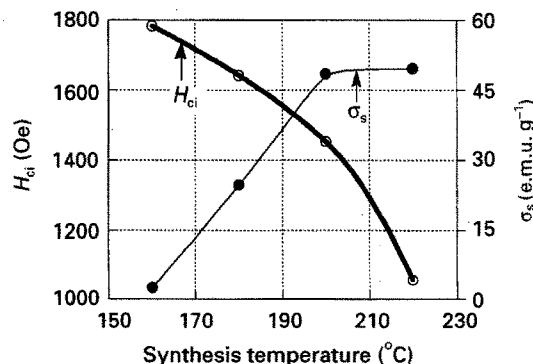


Figure 6 Intrinsic coercivity,  $H_{ci}$ , and saturation magnetisation,  $\sigma_s$ , of strontium hexaferrite, synthesized hydrothermally for 1 h using an  $\text{OH}^-/\text{NO}_3^-$  molar ratio of 2 as a function of temperature.

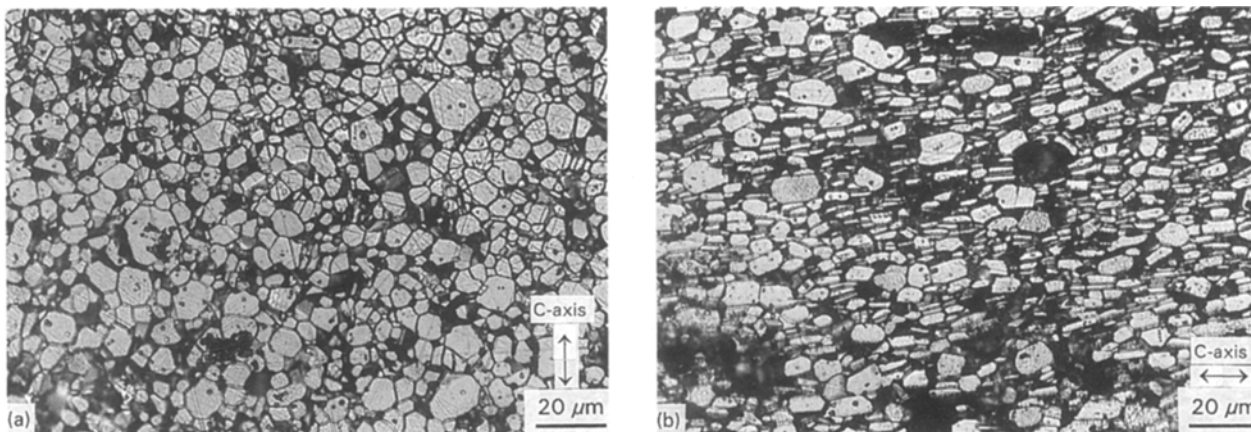


Figure 7 Optical micrograph of wet-pressed and dried sample sintered at 1200°C for 1 h, (a) cut normal to the sample *c*-axis, and (b) cut parallel to the sample *c*-axis.

synthesized hydrothermally for 1 h using an  $\text{OH}^-/\text{NO}_3^-$  molar ratio of 2, as a function of synthesis temperature. The coercivity decreases with increasing synthesis temperature due to a concomitant increase in particle size. In contrast, the saturation magnetization increases linearly with increasing temperature up to 200°C. This significant increase between 160 and 200°C is due to a reduction in the proportion of intermediate phases in the powder. These intermediate phases have been identified previously [11] as  $\alpha\text{Fe}_2\text{O}_3$ ,  $\text{SrFeO}_{2.5}$  and  $\text{Sr}_2\text{FeO}_{4-x}$  using powder X-ray diffraction analysis. However, increasing the synthesis temperature from 200°C to 220°C increases the particle size but has no further significant effect on the particle crystallinity and phase composition as evinced by the unchanging saturation magnetization.

### 3.4. Microstructure and magnetization of sintered $\text{SrFe}_{12}\text{O}_{19}$ magnet samples

Fig. 7a and b show the microstructure of the wet-pressed and dried sample sintered at 1200°C for 1 h perpendicular to the *c*-axis and parallel to the *c*-axis, respectively. Note the plate-like morphology of the strontium hexaferrite grains in Fig. 7b. The magnetization behaviour of the samples sintered at 1200 and 1250°C for 1 h, can be seen in Fig. 8 as a function of the applied field.

Figs 7 and 8 confirm that the fabricated sintered magnets exhibit good alignment of the particles along the sample *c*-axis, and hence, a strongly anisotropic structure. Increasing the sintering temperature from 1200°C to 1250°C has a negligible effect on the sintered density (the density of both samples is about 91% theoretical density), but increases the average grain size, remanence,  $\sigma_r$ , and saturation magnetization,  $\sigma_s$ . The low coercivity of both samples can be attributed to grain growth during sintering. The coercivity may be increased by minimizing grain growth by sintering at a lower temperature and/or shorter time, if necessary by the use of sintering aids such as  $\text{Al}_2\text{O}_3$  and  $\text{SiO}_2$  in appropriate amounts. Characteristics of the samples sintered for 1 h at 1200 and 1250°C, respectively are tabulated in Table III.

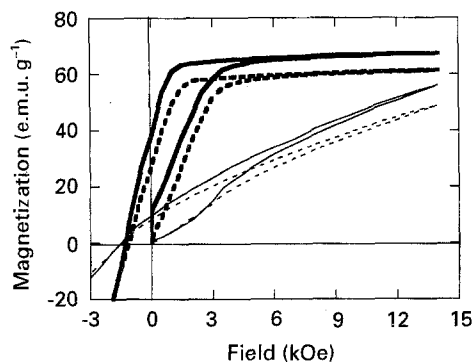


Figure 8 Magnetization curve as a function of applied field for the samples sintered at (---, ----) 1200 and (—, —) 1250°C for 1 h in the (---, —) hard, and (---, —) easy directions.

### 4. Conclusion

The effects of the hydrothermal synthesis conditions (temperature, time and alkali molar ratio) on the magnetic properties of  $\text{SrFe}_{12}\text{O}_{19}$  particles synthesized from nitrate precursors have been investigated. It has been shown that the saturation magnetization,  $\sigma_s$ , remanence,  $\sigma_r$ , and intrinsic coercivity,  $H_{ci}$ , are strong functions of the synthesis conditions. Increasing the synthesis temperature, time and  $\text{OH}^-/\text{NO}_3^-$  molar ratio (up to  $R = 6$ ) decreases  $H_{ci}$  due to the concomitant increase in particle size.  $\sigma_s$  and  $\sigma_r$  are increased on increasing the synthesis temperature from 160°C to 220°C, the synthesis time from 0.25 h to 5 h, and the  $\text{OH}^-/\text{NO}_3^-$  molar ratio from 1.5 to 6, all of which serve to increase the proportion of  $\text{SrFe}_{12}\text{O}_{19}$  present in the powder. Although the particle nucleation and growth rates increase with increasing alkali concentration up to an  $\text{OH}^-/\text{NO}_3^-$  molar ratio of 6, they decrease when the ratio exceeds 6. It was found that optimum magnetic properties could be achieved experimentally when the synthesis temperature, time and  $\text{OH}^-/\text{NO}_3^-$  molar ratio were fixed at 220°C, 2 h and 2, respectively. The fabricated sintered magnets produced from powders synthesized at 220°C for 1 h with an  $\text{OH}^-/\text{NO}_3^-$  of 2 showed a strongly anisotropic structure and good saturation magnetization of 67.26 e.m.u g<sup>-1</sup> (4320 G).

TABLE III Density,  $\rho$ , average grain size,  $d$ , the intrinsic coercivity,  $H_{ci}$ , remanence,  $\sigma_r$ , and saturation magnetization,  $\sigma_s$ , and estimated anisotropy field,  $H_A$ , of the samples sintered at 1200 and 1250 °C for 1 h in the easy and hard directions

Sample	Sintering temp. °C	$\rho$ (g cm <sup>-3</sup> )	$d$ ( $\mu$ m)	$H_{ci}$ easy (hard) (Oe)	$\sigma_r$ easy (hard) (e.m.u. g <sup>-1</sup> )	$\sigma_s$ easy (hard) (e.m.u. g <sup>-1</sup> )	$H_A$ (kOe)
1	1200	4.63	6.0	1127 (1489)	26.87 (8.39)	61.13 (48.7)	18.34
2	1250	4.65	7.8	1284 (1554)	38.55 (9.68)	67.26 (55.96)	17.52

### Acknowledgements

The authors thank the members of the Applied Alloy Chemistry Group (School of Metallurgy and Materials) and the Ceramic Group (IRC/School of Metallurgy and Materials) for their help and cooperation. The provision of facilities by Professor J. F. Knott FRS FEng (Metallurgy and Materials) and Professor M. H. Loretto (IRC) is acknowledged. The financial support of AA by the Iranian government during his PhD studentship is also gratefully acknowledged.

### References

1. H. KOJIMA, in "Ferromagnetic Materials: A Handbook on the Properties of Magnetically Ordered Substances", Vol. 3, edited by E. P. Wohlfarth (North-Holland, Amsterdam, 1982) Ch. 5, pp. 305–91.
2. H. STÄBLEIN, *ibid.*, Vol. 3, Ch. 7, pp. 441–602.
3. SUTARNO, W. S. BOWMAN and G. E. ALEXANDER, *J. Canad. Ceram. Soc.* **39** (1970) 33.
4. S. K. DATE, C. E. DESHPANDE, S. D. KULKARNI and J. J. SHROTRI, in "Proceedings of the 5th International Conference on Ferrites", Bombay, India, 10–13 Jan., 1989, edited by C. M. Srivastava and M. J. Patni (1990) pp. 55–60.
5. V. V. PANKOV, M. PERNET, P. GERMI and P. MOLLARD, *J. Magn. Magn. Mater.* **120** (1993) 69.
6. K. HANEDA, C. MIYAKAWA and K. GOTO, *IEEE Trans. Magn. MAG* **23** (1987) 3134.
7. D. BAHADUR and D. CHAKRAVORTY, in "Proceedings of the International Conference on Ferrites", India (1989) pp. 189–93.
8. H. SATO and T. UMEDA, *J. Mater. Trans.* **34** (1) (1993) 76.
9. R. J. ROUTIL and D. BARHAM, *J. Canad. Chem.* **52** (1974) 3235.
10. C. H. LIN, Z. W. SHIH, T. S. CHIN, M. L. WANG and Y. C. YU, *IEEE Trans. Magn. MAG* **26** (1990) 15.
11. A. ATAIE, I. R. HARRIS and C. B. PONTON, in British Ceramic Proceedings **52**, Electroceramics: Production, Properties and Microstructures", Proceedings of a Symposium held as part of the Condensed Matter and Materials Physics Conference, University of Leeds, 20–22 December 1993, edited by W. E. Lee and A. Bell (Institute of Materials, London, 1994) pp. 273–81.
12. A. ATAIE, M. R. PIRAMOON, C. B. PONTON and I. R. HARRIS, *J. Mater. Sci.* December, 1994.

Received 11 July  
and accepted 11 August 1994